


## RESEARCH ARTICLE

# Minimally invasive manganese-enhanced magnetic resonance imaging for the sciatic nerve tract tracing used intra-articularly administered dextran–manganese encapsulated nanogels

Yawara Eguchi<sup>1</sup>  | Shuhei Murayama<sup>2</sup> | Hirohito Kanamoto<sup>3</sup> | Koki Abe<sup>3</sup> | Masayuki Miyagi<sup>4</sup> | Kazuhisa Takahashi<sup>3</sup> | Seiji Ohtori<sup>3</sup> | Ichio Aoki<sup>5,6</sup>

<sup>1</sup>Department of Orthopaedic Surgery, Shimoshizu National Hospital, Chiba, Japan

<sup>2</sup>Department of Bioanalytical Chemistry, School of Pharmacy, Showa University, Tokyo, Japan

<sup>3</sup>Department of Orthopaedic Surgery, Graduate School of Medicine, Chiba University, Chiba, Japan

<sup>4</sup>Department of Orthopaedic Surgery, School of Medicine, Kitasato University, Sagami-hara, Japan

<sup>5</sup>Department of Molecular Imaging and Theranostics, National Institute of Radiological Sciences (NIRS)

<sup>6</sup>Institute for Quantum Life Science, National Institutes for Quantum and Radiological Science and Technology (QST), Chiba, Japan

## Correspondence

Ichio Aoki, Institute for Quantum Life Science (iQLS), National Institutes for Quantum and Radiological Science and Technology (QST), 4-9-1 Anagawa, Inage, Chiba Japan.  
Email: aoki.ichio@qst.go.jp; iaoki.jp@gmail.com

## Funding information

Center of Innovation Program; Nakatomi Foundation; Mitsui Sumitomo Insurance Welfare Foundation

## Abstract

Manganese-enhanced magnetic resonance imaging (MEMRI) enables tract tracing to follow neural pathways through axonal transport. However, the method is problematic because of the high local concentrations of Mn<sup>2+</sup> involved. We developed a tetrananogel containing a dextran-manganese complex (Dex-Mn-Gel) and applied this nanogel to rats. MnCl<sub>2</sub> (n = 5), Dex-Mn-Gel (n = 5), or saline control (n = 3) was injected into the left knee joint of the rats (n = 13). Inflammation and tissue alterations in the knee joint were also evaluated histologically. T1-weighted images were obtained on a 7 T MRI system 24 hours after the administration and compared across groups. The sciatic nerve in both legs and the surrounding musculature were used as regions of interest (ROI). No swelling was found in the knee joint infused with Dex-Mn-Gel, although prominent swelling of the knee joint was observed with MnCl<sub>2</sub>. White blood cells inside the knee joint tissue infused with the Dex-Mn-Gel were significantly less abundant (45%, *P* < .05) compared with the knee joints infused with MnCl<sub>2</sub>. Visualization of the sciatic nerve was significantly enhanced in rats treated with both forms of Mn<sup>2+</sup> compared with controls (*P* < .01). This study is the first to attempt intra-articular administration of a manganese contrast agent into joint-capsule and demonstrate tract visualization. The Dex-Mn-Gel can be taken up by the nerve endings and reduce Mn<sup>2+</sup> toxicity. Dex-Mn-Gel will provide a minimally invasive method for visualizing nerve tracts in vivo.

## KEYWORDS

knee joint, MEMRI, nanogels containing Dex-Mn complex, retrograde tract tracing, sciatic nerve

## 1 | INTRODUCTION

As our society ages, suffering from musculoskeletal pain, often characterized as aging-related back pain or joint pain, will become more frequent. However, we have yet to elucidate the mechanism whereby

**ABBREVIATIONS:** Dex-Mn-Gel, tetra-nanogel containing dextran-manganese complex; MEMRI, manganese-enhanced magnetic resonance imaging.

Yawara Eguchi, Shuhei Murayama, and Hirohito Kanamoto contributed equally to the study.

This is an open access article under the terms of the Creative Commons Attribution-NonCommercial License, which permits use, distribution and reproduction in any medium, provided the original work is properly cited and is not used for commercial purposes.

© 2019 The Authors. JOR Spine published by Wiley Periodicals, Inc. on behalf of Orthopaedic Research Society

such pain becomes chronic, and treatment for these conditions has not been clearly established. The stimulation of local nociceptors is transmitted through peripheral nerves, such as the sciatic nerves, up the spine to the brain where stimuli are perceived as pain. The elucidation of pain pathways in animal models has primarily focused on the use of immunohistological methods with nerve tracers such as Fluoro-Gold.<sup>1,2</sup> Several studies have utilized retrograde transport of Fluoro-Gold in rats to show that sensory fibers from the T12 to L6 dorsal root ganglia (DRGs) innervate to the L5 to L6 intervertebral disc<sup>1</sup> and fibers from L4 DRGs extend to the knee joint.<sup>2</sup> However, a visualization method for these pathways in living animals has yet to be established.

If nerve tract tracing could be realized *in vivo*, and if pain transmission pathways could be visualized and analyzed in a minimally invasive manner, then, we will have gained a powerful index for the diagnosis and treatment of chronic pain, such as selective nerve root infiltration.

Recent improvement of magnetic resonance imaging (MRI) devices, such as multichannel detection and improved pulse sequences, has allowed high resolution three-dimensional (3D) imaging with a shorter scanning time. Evaluation of peripheral nerve function or anatomy using MRI has been described, including blood-oxygen-level dependent (BOLD)-based functional MRI (fMRI) in the brain<sup>3</sup> and spinal cord,<sup>4</sup> and diffusion tensor imaging of the spine and peripheral nerves.<sup>5</sup> However, fMRI lacks spatial resolution and relies on the secondary response of blood flow, and diffusion tensor-based tract estimation cannot identify the nerve endings and the direction of the axonal transport microscopically. Manganese is an effective contrast agent that shortens longitudinal relaxation time (T1) and enhances the positive signal in T1-weighted images. When Mn<sup>2+</sup> is administered either locally or systemically, axonal transport can be followed or visualized through tract tracing (manganese-enhanced MRI: MEMRI) in the periphery<sup>6,7</sup> and in the brain.<sup>8,9</sup> MEMRI can be classified three types such as activity-induced MEMRI (AIM MRI) with blood-brain barrier disruption,<sup>10</sup> tract tracing with local administration,<sup>6,7</sup> and neuroarchitectural/functional MEMRI with systemic administration.<sup>11</sup> In tract tracing<sup>6,7</sup> involves subcutaneous or local administration of Mn that is transported through axonal transport allowing visualization of nerve tracts in the peripheral nerves and inside the brain. However, no papers have reported any success in a noninvasive trace of the sciatic nerve pathway.

However, most previous reports of MEMRI are confined to limited pathways: for example, through nasal mucosa for olfactory nerve tracing, or intraocular administration for optic nerve tracing, and few reports cover sciatic nerve tracing.<sup>12,13</sup> To trace nerve tracts, MEMRI requires high local concentrations of MnCl<sub>2</sub> (100-4000 mM) to obtain sufficient contrast. These concentrations of MnCl<sub>2</sub>, however, are toxic to the local administration site<sup>14</sup> and the large difference in ion concentrations leads to serious swelling, particularly in tissue where it can diffuse, such as in muscle. Therefore, tract tracing using MEMRI has been applied in limited "isolated" areas, such as the ophthalmic or nasal cavities, where structures allow an "endogenous controlled-release" of the contrast agent into the nerve endings.<sup>15</sup>

We hypothesized that a tetrananogel containing a dextran-manganese complex (Dex-Mn-Gel) could reduce tissue toxicity at the injection site with sufficient contrast capabilities for visualizing the nerve tract. In the present study, we developed a Dex-Mn-Gel to enable minimally invasive peripheral nerve tract tracing by MRI. A dextran molecule was bound to several Mn<sup>2+</sup>-chelates and the dextran-Mn was enmeshed at high concentrations within the structure of a nanoparticle gel. Many sciatic nerve endings are distributed throughout the joint capsule.<sup>2</sup> We administered the prepared Dex-Mn-Gel contrast agent into the knee joint of rats to visualize the sciatic nerve that originates in the knee joint in a minimally invasive manner. The knee joint capsule is isolated from other surrounding structures and can prevent diffusion of the injected Dex-Mn-Gel. Dex-Mn-Gel-based MEMRI may contribute to the elucidation of pain transmission pathways such as in the spinal cord or dorsal root ganglia innervating the knee joint. Here, we demonstrate that Dex-Mn-Gel-based MEMRI avoids toxicity at the injection site and can enable visualization of the sciatic nerve tract in a minimally invasive manner *in vivo*.

## 2 | METHODS

All protocols for animal procedures were reviewed and approved by the animal care and use committee of the National Institute of Radiological Sciences, Chiba-City, Japan, and followed the National Institutes of Health Guidelines for the Care and Use of Laboratory Animals.

### 2.1 | Intra-articular manganese injection

Thirteen 6-week-old Sprague Dawley (SD) rats (body weight: 250-300 g, Japan SLC, Tokyo, Japan) were used. Contrast agents (MnCl<sub>2</sub> or Dex-Mn-Gel) were injected into the left knee joints of these rats under isoflurane inhalation anesthesia (1.5%-2.0%, Escain, Mylan, Tokyo, Japan). The contrast agent was injected through the patellar ligament using a 27-gauge needle with the leg flexed at a 90° angle at the knee. A group administered MnCl<sub>2</sub> (100 mM, 50 µL, n = 5), a group administered Dex-Mn-Gel (100 mM, 50 µL, n = 5), and a vehicle control group (n = 3) were compared. The MnCl<sub>2</sub> was dissolved in water and adjusted iso-osmotically using saline.<sup>6</sup> After the administration, the local injected area was confirmed using MRI. The knee joint image was enhanced 24 hours after administration of MnCl<sub>2</sub> into the joint capsule (Figure 1A).

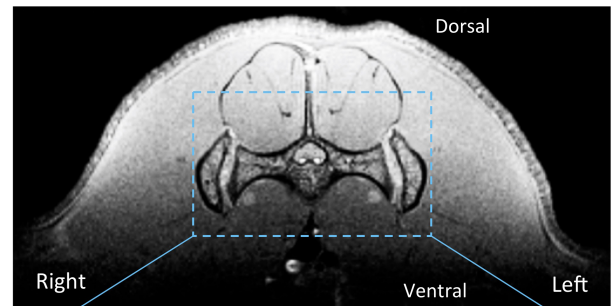
### 2.2 | Manganese-enhanced MRI

T1-weighted images were obtained using 7 T MRI 24 hours after contrast agent injection. Rats were anesthetized using isoflurane (1.5%-2.0%, Escain, Mylan) and immobilized in the supine position in the center of an MRI bore. The rectal temperature was maintained at 36°C to 37°C. All MRI data were acquired on a 7 T MRI system (Magnet: Kobelco, Japan; Console: Bruker Biospin, Avance I,

**FIGURE 1** Sagittal magnetic resonance images of the knee joint (A), axial images of the entire pelvis and both legs (B), and an enlarged picture of the sciatic nerve in the vicinity of the pelvic bone (C) after administering  $MnCl_2$ . The knee joint was enhanced at 24 hours after  $MnCl_2$  administration into the joint capsule. The arrow indicates the contrast effect in the knee joint (A). Ant indicates anterior and Post indicate posterior. The sciatic nerve in the transaxial T1-weighted image (red circle) and surrounding muscle (white circle) were set as regions of interest (ROI). The normalized signal intensity ratio was calculated as the intensity of the sciatic nerve divided by the intensity in the muscle (C)



(B) Sciatic nerve in the vicinity of the pelvic bone



Germany) equipped with a gradient system (BGA12, Bruker Biospin), in combination with a volume coil (inner diameter 72 mm, Bruker) for transmission and a two-channel phased-array surface coil (Rapid Biomedical, Germany) for signal reception. For the T1-weighted MRI, the following parameters were used: spin-echo method, repetition time (TR) = 400 ms, echo time (TE) = 9.6 ms, field of view (FOV) =  $38.4 \times 19.2$  mm<sup>2</sup>, matrix size =  $256 \times 128$ , slice thickness = 1 mm, slice gap = 2.0 mm, and 5 slices. The inhomogeneity in sensitivity of the surface coil was corrected using an AFNI software tool (3dUnifize, NIMH, NIH, USA). Regions of interest (ROI) included the sciatic nerve on both sides of the pelvis, and surrounding musculature. The normalized signal ratio was calculated as the intensity of the sciatic nerve divided by the intensity in the same muscle slice (Figure 1B).

### 2.3 | Preparation of the PEG-Ac monomer, DAB-Ac monomer, and Dex-Mn

Tetra-poly(ethyl glycol)-amine (Sunbright PTE-050PA; Mn, 5328 g/mol) was purchased from NOF Corporation (Tokyo, Japan). *N,N,N',N'*-tetramethylethylenediamine (TEMED), dichloromethane, acryloyl chloride, triethylamine, ammonium persulfate (APS), hydrochloric acid, methanol, and diethyl ether were purchased from Wako Pure Chemical Industries (Osaka, Japan). Dimethyl sulfoxide, 2-morpholineethanesulfonic acid and 4-dimethylaminopyridine (DMAP) were obtained from Nacalai Tesque (Kyoto, Japan). Dextran with a weight-averaged molecular weight of 40 000 (Dex), diethylenetriaminepentaacetic acid (DTPA) anhydride, manganese chloride, first generation polypropylenimine tetramine dendrimer (DAB-Am-4), and rhodamine 6G were purchased from Sigma-Aldrich (St. Louis, Missouri). Water was purified with a Milli-Q apparatus

(Millipore, Bedford, Massachusetts). A detailed materials preparation protocol has been published previously.<sup>16-18</sup>

### 2.4 | Preparation of the nanogels containing Dex-Mn complex

Tetrananogels containing Dex-Mn-DOTA<sup>15</sup> were prepared using a modified method for nanogels containing proteins.<sup>17,19</sup> The gel material, PEG-Ac, was synthesized by condensation reactions between tetra-PEG-amine and acryloyl chloride. The reacted product was precipitated in diethyl ether on ice, and the suspension was filtered, then dialyzed to purify the PEG-Ac. The structure of PEG-Ac was confirmed by <sup>1</sup>H NMR.<sup>16</sup>

A mixture of 200  $\mu$ L of 100 mg/mL the PEG-Ac, 50  $\mu$ L of 400 mM ( $Mn^{2+}$ ) Dex-Mn, 50  $\mu$ L of 16 mg/mL DAB-Ac, 50  $\mu$ L of 2 mg/mL of rhodamine, 25  $\mu$ L of 0.1 mM APS, and 25  $\mu$ L of 0.1 mM TEMED was stirred for 20 minutes at room temperature. The 3D polymer mesh structure of the gel entraps the Dex-Mn. After the reaction, the products were recovered using a Vivaspin 6 concentrator with a MWCO of 30 000 (Sartorius, Germany) at 6000 g for 15 minutes at 4°C. Water was added to adjust gels to a final concentration of 100 mM  $Mn^{2+}$  in gel solution.

### 2.5 | Properties of the nanogels

The nanogel containing concentrates were analyzed using a dynamic light scattering (DLS) system (Zetasizer Nano ZS, Malvern, Westborough, Massachusetts). Concentrated nanogel solutions containing Dex-Mn were stored. After 1 day, nanogel solutions were reconcentrated using a Vivaspin 6 concentrator with a MWCO of

30 000. The relaxivities of the concentrate and filtrate were measured on a 1 T-MRI system (ICON, Bruker-Biospin) with a solenoid coil.

## 2.6 | Histopathology of the knee joint

The soft tissues around each side of the joint and cartilage including the synovium and capsule were resected under deep anesthesia. Thereafter, the animal was euthanized. The resected limbs were cut at midfemur and midtibia and immersed in buffered paraformaldehyde fixative at 4°C for 1 week. The specimens were demineralized by K-CX (Falma, Tokyo, Japan) for 24 hours and the formalin fixed-paraffin embedded tissue sections were prepared using standard histological techniques. Tissue sections were stained using hematoxylin and eosin (HE), and assessed by light microscopy.

## 2.7 | Determination of white blood cell count in knee joint tissue

After HE staining, five random photos each of microscopic field view of the Control (right knee, non-enhanced side,  $n = 5$ ), Dex-Mn-Gel group (left knee;  $n = 3$ ), and  $MnCl_2$  groups (left knee,  $n = 3$ ) were taken at 100× (BX-41, Olympus, Tokyo, Japan) with a Moticam Pro 252A camera (Shimadzu, Kyoto, Japan). All soft tissues within the joint, with the exception of bone, cartilage and tendon tissues, were measured. Image analysis software (WinROOF version 7.2, Mitani-shoji, Fukui, Japan) was used to check cell morphology to count all white blood cells (WBC) including those within the vasculature. Actual areas of each image were also measured to determine the WBC count per  $mm^2$ .

## 2.8 | Statistical analysis

Statistical analyses were performed using by SAS for Windows (Ver. 9.4, SAS Institute Inc., Cary, North Carolina). An Analysis of variance (ANOVA) followed by a post hoc test using the Bonferroni method was used to compare parameters between each group;  $P < .05$  was considered significant. All data are expressed as the mean  $\pm$  SD.

## 3 | RESULTS

### 3.1 | Toxicity of $Mn^{2+}$ in the knee joint capsule and its suppression

To achieve minimally invasive MEMRI tract tracing of the sciatic nerve, the Dex-Mn-Gel was prepared as a 120 nm nanogel, which was measured by DLS, and injected into the knee joint capsule. The knee joint showed swelling on the side administered 100 mM  $MnCl_2$  (Figure 2C). In contrast, there was no difference between the side administered Dex-Mn-Gel and the normal side (Figure 2B). For the evaluation of swelling, we calculated the diameter ratio of the knee joint as the administered/normal side in the two-dimensional (2D) horizontal images. The diameter ratio of swelling in the knee in the  $MnCl_2$  group was 1.5, which was a significant increase compared to the control (1.0) and Dex-Mn-Gel (1.1) groups ( $P < .05$ ). WBC infiltration at the knee joint was also evaluated using H&E staining (Figure 3). Tissue alterations were observed in rats administered  $MnCl_2$  (Figure 3A). WBC infiltration was increased in both the group administered Dex-Mn-Gel ( $1582.5 \pm 207.1$  cells/ $mm^2$ ) and in the group administered  $MnCl_2$  ( $3550.4 \pm 629.8$  cells/ $mm^2$ ) compared with the saline vehicle control ( $382.9 \pm 97.7$  cells/ $mm^2$ ). WBC counts in the group administered  $MnCl_2$  were approximately 10-fold higher than in the controls and this difference was significant ( $P < .001$ ). By contrast, WBC counts in the group administered Dex-Mn-Gel were half that of the  $MnCl_2$  group and were significantly less than in the group administered  $MnCl_2$  ( $P < .001$ ) (Figure 3B).

We designed and prepared Dex-Mn-Gel, which encapsulated Dex-Mn in the 3D polyethylene glycol mesh of its nanogel structure to reduce the local  $Mn^{2+}$  concentration. The mesh structure restricted the movement of the encapsulated Dex-Mn, isolated it from the surrounding environment, and minimized inflammation. The stability of the Mn contrast agent ( $Mn^{2+}$  or Dex-Mn) inside the gel was estimated in vitro. The results indicated that very little of the Dex-Mn leaked into the solution from the gel within 24 hours (Table 1).

### 3.2 | Manganese enhancement of the sciatic nerve tract

We evaluated MRI contrast enhancement of the sciatic nerve after  $MnCl_2$  or Dex-Mn-Gel injection into the unilateral knee joint. The sciatic nerve in rats infused with either the Dex-Mn-Gel or  $MnCl_2$  was

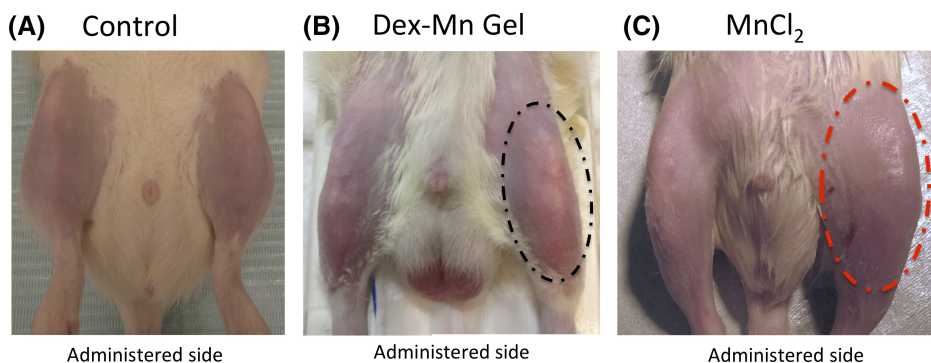


**FIGURE 2** Knee joint findings. Swelling was noted in the left knee (contrast-enhanced side) after administering  $MnCl_2$  (C; red dotted line), while the left knee joint (contrast-enhanced side) did not show swelling after administration of the Dex-Mn-Gel (B; black dotted line) or saline (A). The evaluations of knee joint finding were performed 24 hours after contrast agent injection

**FIGURE 3** Hematoxylin and eosin staining (A) and white blood cell counts (B). White blood cell infiltration was noted in knees injected with either the Dex-Mn-Gel or  $MnCl_2$  compared with controls. Upper row indicated the high magnification images and lower row indicated the high magnification images of the same field. However, the infiltration was more prominent in the knees injected with  $MnCl_2$  than those with the Dex-Mn-Gel. The white blood cell counts (cell number/ $mm^2$ ) were as follows: control group,  $382.9 \pm 97.7$ ; Dex-Mn-Gel group,  $1582.5 \pm 207.1$ ;  $MnCl_2$  group,  $3550.4 \pm 629.8$ . The  $MnCl_2$  group showed 10-fold higher counts and the Dex-Mn-Gel group showed 4-fold higher counts compared with the control group ( $P < .001$ ). Tissue inflammation in the Dex-Mn-Gel group was half of that in the  $MnCl_2$  group ( $P < .001$ )

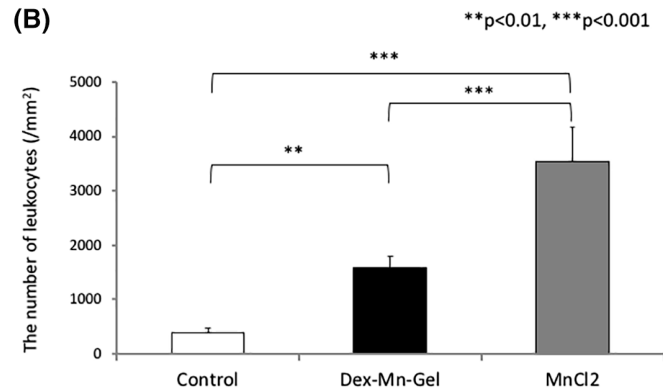
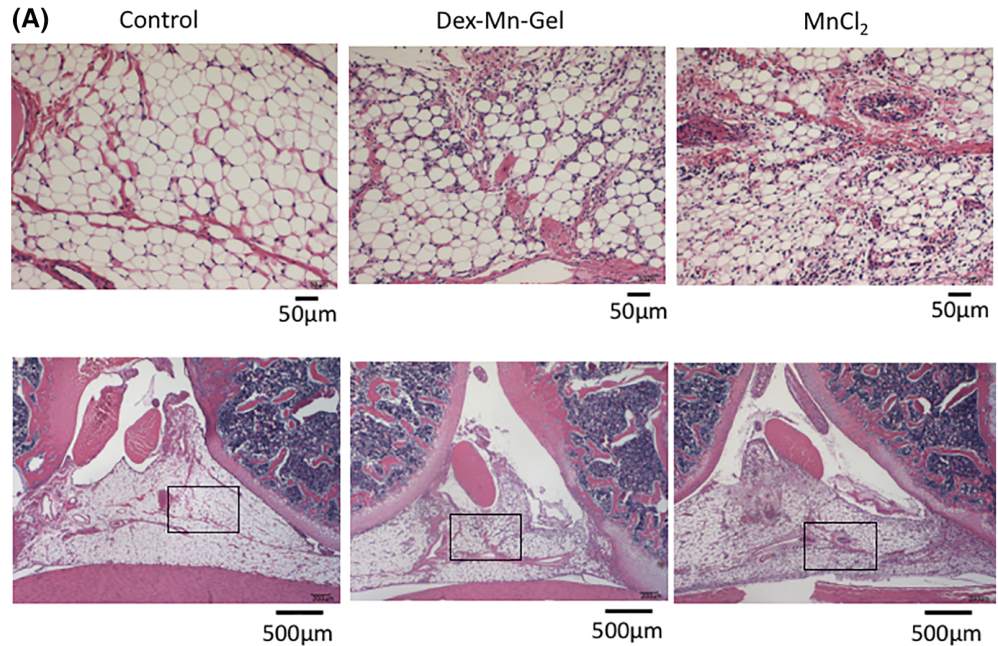


**TABLE 1** Longitudinal relaxation rate of the Dex-Mn-Gel solution and the solvent 24 hours after preparation

[Mn] (mM)	Longitudinal relaxation rate at 1 T, 23° C ( $s^{-1}$ )	
	Dex-Mn-Gel solution	Solvent after Dex-Mn-Gel removed (24 h) <sup>a</sup>
0	0.46	0.47
1.25	6.95	0.47
2.50	12.34	0.47
5.00	20.42	0.48

<sup>a</sup>To evaluate  $Mn^{2+}$  or Dex-Mn leakage from the Gel to the solvent, different concentrations of the Dex-Mn-Gel were removed from the solvents 24 hours after preparation and the relaxation times of solvents without the Dex-Mn-Gel were measured.

clearly enhanced in T1-weighted imaging (Figure 4). The sciatic nerve pathway was visualized clearly from the proximal knee joint distally to the vicinity of the pelvic bone with MEMRI using the minimally invasive Dex-Mn-Gel-based method (Figure 5).

Normalized signal ratios in the control group were  $1.13 \pm 0.02$ , and those in the group administered Dex-Mn-Gel were  $1.27 \pm 0.09$

(Dex-Mn-Gel side) and  $1.26 \pm 0.08$  (contralateral sides), and those in the group administered  $MnCl_2$  were  $1.30 \pm 0.07$  ( $MnCl_2$  side) and  $1.20 \pm 0.04$  (contralateral sides). In the treated leg, the sciatic nerve showed significantly higher contrast after  $MnCl_2$  ( $P < .001$ ) and Dex-Mn-Gel ( $P < .01$ ) administration than untreated controls (Figure 6). Surprisingly, a small enhancement in the non-injected leg was also observed both in the  $MnCl_2$  and Dex-Mn-Gel treated rats (Figure 6). We also performed a longitudinal measurement ( $n = 1$ ) after  $MnCl_2$  administration into the joint capsule. Figure 7 showed normalized signal ratio which was normalized to the signal intensity at 0 hour. There was little signal increase in either the ipsilateral or contralateral sciatic nerves 1 to 4 hours after  $MnCl_2$  administration, and the signal in the ipsilateral side (1.147) increased higher than in the contralateral side (1.061) 24 hours after  $MnCl_2$  administration, suggesting that the blood flow route is not a predominant contributor to contralateral side enhancement.

## 4 | DISCUSSION

$MnCl_2$  injected into the knee joint clearly enhanced imaging of the sciatic nerve tract. This indicates that MEMRI can be used for the visualization of sciatic nerve tracers. Dextran-conjugated fluorescent dyes

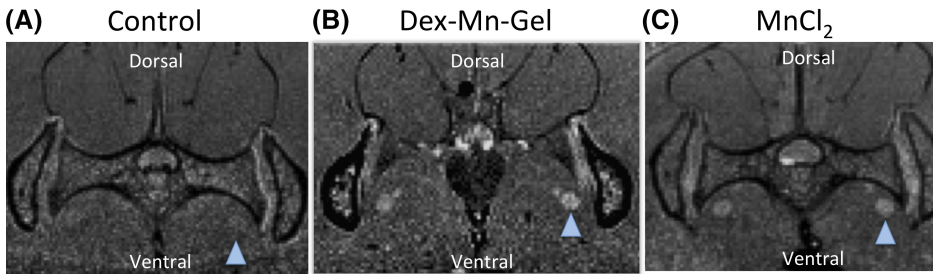


**FIGURE 4** Axial images of the sciatic nerve in the vicinity of the pelvic bone. The left sciatic nerve (Mn treated side) was enhanced 24 hours after Dex-Mn-Gel (B) and MnCl<sub>2</sub> (C) (arrowhead) administration in the joint capsule compared to Controls (A)

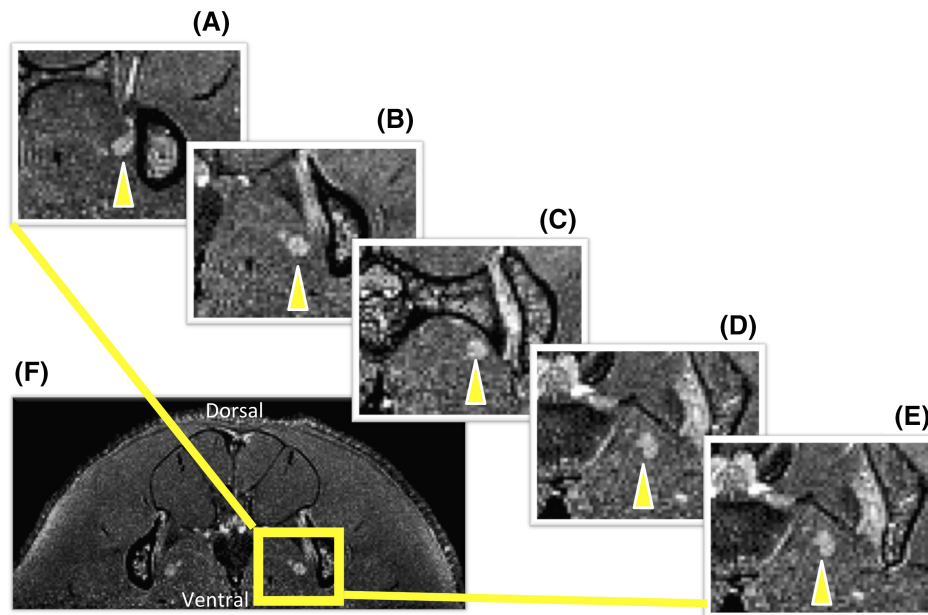


**FIGURE 5** Axial magnetic resonance images of the sciatic nerve in the vicinity of the pelvic bone enhanced with the Dex-Mn-Gel (F). The sciatic nerve pathway (Mn-treated side) was visualized clearly from the proximal (A) to distal (E) pelvic bone. The arrowheads indicate the sciatic nerves

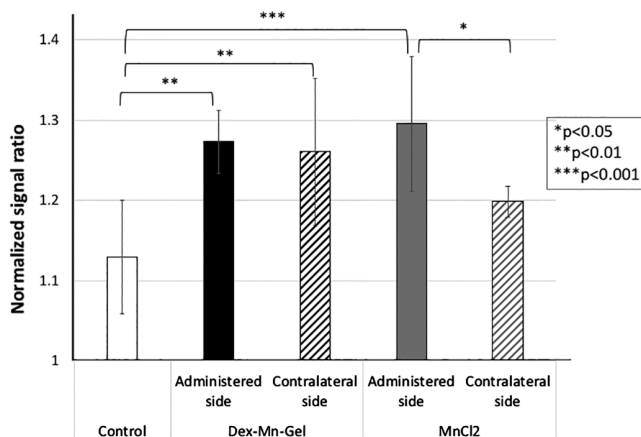


**FIGURE 6** Signal intensity normalized to muscle. The normalized signal intensity in the control group was  $1.129 \pm 0.019$ . In the Dex-Mn-Gel group, intensities were  $1.272 \pm 0.090$  on the Dex-Mn-Gel side and  $1.260 \pm 0.083$  on the contralateral side. In the MnCl<sub>2</sub> group, intensities were  $1.295 \pm 0.070$  on the MnCl<sub>2</sub> side and  $1.198 \pm 0.039$  on the contralateral side. The signal intensity in both the MnCl<sub>2</sub> group ( $P < .001$ ) and the Dex-Mn-Gel group ( $P < .01$ ) was significantly higher than in the control group

have been demonstrated to act as tract tracers for peripheral nerves.<sup>20</sup> Thus, Dex-Mn-Gel nanoparticles can also be taken up by the peripheral nerves in addition to the small amount of released Mn<sup>2+</sup>. We were surprised that there was enhancement on both the injected and contralateral side of the sciatic nerve. Although the mechanism remains unclear, we presume that the contralateral side was enhanced through spinal cord transport and partly through blood flow when the injection procedure into the joint capsule was imperfect. The Dex-Mn-Gel-enhanced visualization of the sciatic nerve tract to a contrast level similar to that found with MnCl<sub>2</sub>, although with lower toxicity. MEMRI and gel-based polymeric dose optimization will minimize the invasiveness of neural pathway tracing because of the restricted-release properties of the polymer, and may open a route to future clinical applications.

#### 4.1 | Sciatic nerve tract tracing

MEMRI has been studied in a model of sciatic nerve injury in rats using local injection of MnCl<sub>2</sub> into the sciatic nerve<sup>12</sup> or peritoneum.<sup>13</sup> MnCl<sub>2</sub> administered into the sciatic nerve behaves as a retrograde

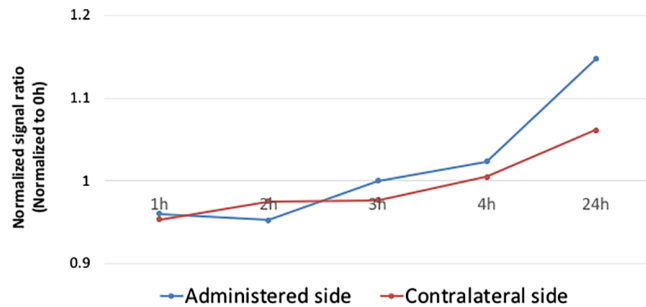


**FIGURE 7** Longitudinal measurement (1-24 hours) showing normalized signal ratio which was normalized to 0 hour after  $\text{MnCl}_2$  administration into the joint capsule. There is little longitudinal signal increase in either the ipsilateral or contralateral sciatic nerves 1-4 hours after  $\text{MnCl}_2$  administration, and the signal in the ipsilateral side (1.147) increased higher than in the contralateral side (1.061) 24 hours after  $\text{MnCl}_2$  administration

axonal tracer and the signal intensity has been shown to correlate significantly with a behavioral functional test outcome.<sup>9</sup> Increased  $\text{Mn}^{2+}$  uptake in the lumbar plexus after intraperitoneal administration of  $\text{Mn}^{2+}$ , which correlated with the development of allodynia, was shown in a model of neuropathic pain.<sup>13</sup> To the best of our knowledge, until now there has been no previous study that has visualized the tract of the sciatic nerve from the knee joint using an MRI tracer.

## 4.2 | Potential benefits and issues with Dex-Mn-Gel use

There is currently just one  $\text{Mn}^{2+}$ -chelate-based contrast agent, Mn-dipyridoxyl-di-phosphate (MnDPDP, Teslascan, Mangafodipir, GE Healthcare), which is clinically approved for liver imaging in humans.<sup>21</sup>  $\text{Mn}^{2+}$ -“divalent ion”-based MEMRI is problematic in clinical applications because of its local<sup>15</sup> and cardiac toxicity. PEG-based tetrananogels are rapidly excreted in the urine after intravenous administration.<sup>17</sup> Thus, encapsulation within a nanogel reduces the risk of high concentrations of  $\text{Mn}^{2+}$ .

The release of a variety of molecules (such as proteins) can be controlled with the use of nanogels, by physically trapping compounds within the mesh structure of the tetrananogel.<sup>18</sup> Dex-Mn-Gel has potential not only as a minimally invasive tract tracer, but as a controllable therapeutic platform in vivo.

For more efficient signal enhancement, the chelate structure of  $\text{Mn}^{2+}$  should be optimized. Although our DOTA-based Dex-Mn showed good stability in solution (Table 1), the relaxivity of the DOTA-Mn is not high in comparison to other chelates for  $\text{Mn}^{2+}$ .<sup>22</sup> In future research, an optimized chelate for  $\text{Mn}^{2+}$  with the Dex-Gel will isolate the nerve tract clearly and provide better contrast.

Advances in molecular biology methods have led to reporting of various mechanisms for the transmission of pain in musculoskeletal sensory pathways, but the mechanism underlying chronic musculoskeletal pain has yet to be fully elucidated, and treatment policies have not yet been clearly established. Dex-Mn-Gel-based MEMRI will not only contribute to visualize the neural pathways and function but

may also suggest treatment strategies for pain through the quantitative manganese transfer index.<sup>23</sup> In future studies, we will aim to further improve the safety of this method, evaluate toxicity, conduct 3D observation methods including the spinal cord, and apply our methods to various animal models of chronic musculoskeletal pain, such as models of nerve injury and knee joint injury, to advance the clinical potential of these methods.

In summary, we successfully visualized the sciatic nerve pathway in rats with MEMRI using a minimally invasive Dex-Mn-Gel-based method. Contrast-enhanced sciatic nerves were observed after administering the gel into knee joints. The 3D polymer mesh structure containing Dex-Mn allows for restricted release of the Dex-Mn contrast agent, which greatly reduces tissue toxicity compared with unencapsulated  $\text{Mn}^{2+}$  contrast agent. Thus, Dex-Mn-Gel-based MEMRI will provide a minimally invasive method for visualizing nerve tracts. Reduced leakage of Mn from nanogels may open the door to clinical applications after careful evaluation of their long-term toxicity and clearance of released Mn.

## ACKNOWLEDGMENTS

This study was supported in part by AOSpine Japan Research (application number AOSJP[R]2015-03), Mitsui Sumitomo Insurance Welfare Foundation, the Nakatomi Foundation, ZENKYOREN (National Mutual Insurance Federation of Agricultural Cooperatives), and JSPS KAKENHI grant numbers 26860032 and 17H00860. The authors thank Sayaka Shibata, Nobuhiro Nitta, Sayaka Hayashi, and Yoshikazu Ozawa (QST, NIRS) for help with the animal and MRI experiments. The MRI research was supported in part by the Center of Innovation Program (COI stream from JST) and by AMED under Grant Number 16cm0106202h and 17dm0107066h.

## CONFLICT OF INTERESTS

The authors declare no competing financial interests.

## AUTHOR CONTRIBUTIONS

Y.E., S.M., K.T., S.O., and I.A. were responsible for the conception and design of the study. Y.E., and I.A. drafted the manuscript. Y.E., S.M., H.K., K.A., and M.M. performed the data analysis. All authors participated in interpretation of the findings and all authors read and approved the final version of the manuscript. All authors confirm that the content has not been published elsewhere and does not overlap with or duplicate their published work.

## ORCID

Yawara Eguchi  <https://orcid.org/0000-0003-2247-5376>

## REFERENCES

1. Ohtori S, Takahashi Y, Takahashi K, et al. Sensory innervation of the dorsal portion of the lumbar intervertebral disc in rats. *Spine*. 1999;24(22):2295-2299.
2. Orita S, Ishikawa T, Miyagi M, et al. Pain-related sensory innervation in monoiodoacetate-induced osteoarthritis in rat knees that gradually develops neuronal injury in addition to inflammatory pain. *BMC Musculoskelet Disord*. 2011;12:134.
3. Ogawa S, Lee TM, Kay AR, Tank DW. Brain magnetic resonance imaging with contrast dependent on blood oxygenation. *Proc Natl Acad Sci U S A*. 1990;87(24):9868-9872.
4. Majcher K, Tomanek B, Tuor UI, et al. Functional magnetic resonance imaging within the rat spinal cord following peripheral nerve injury. *Neuroimage*. 2007;38(4):669-676.
5. Takagi T, Nakamura M, Yamada M, et al. Visualization of peripheral nerve degeneration and regeneration: monitoring with diffusion tensor tractography. *Neuroimage*. 2009;44:884-892.
6. Silva AC, Lee JH, Aoki I, Koretsky AP. Manganese-enhanced magnetic resonance imaging (MEMRI): methodological and practical considerations. *NMR Biomed*. 2004;17(8):532-543.
7. Olsen Ø, Thuen M, Berry M, et al. Axon tracing in the adult rat optic nerve and tract after Intravitreal injection of MnDPDP using a semiautomatic segmentation technique. *J Magn Reson Imaging*. 2008;27(1):34-42.
8. Saleem KS, Pauls JM, Augath M, et al. Magnetic resonance imaging of neuronal connections in the macaque monkey. *Neuron*. 2002;34:685-700.
9. Van der Linden A, Verhoye M, Van Meir V, et al. In vivo manganese-enhanced magnetic resonance imaging reveals connections and functional properties of the songbird vocal control system. *Neuroscience*. 2002;112:467-474.
10. Inoue Y, Aoki I, Mori Y, et al. Detection of necrotic neural response in super-acute cerebral ischemia using activity-induced manganese-enhanced (AIM) MRI. *NMR Biomed*. 2010 Apr;23(3):304-312.
11. Aoki I, Wu YJ, Silva AC, Lynch RM, Koretsky AP. In vivo detection of neuroarchitecture in the rodent brain using manganese-enhanced MRI. *Neuroimage*. 2004 Jul;22(3):1046-1059.
12. Matsuda K, Wang HX, Suo C, et al. Retrograde axonal tracing using manganese enhanced magnetic resonance imaging. *Neuroimage*. 2010;50(2):366-374.
13. Behera D, Behera S, Jacobs KE, Biswal S. Bilateral peripheral neural activity observed in vivo following unilateral nerve injury. *Am J Nucl Med Mol Imaging*. 2013;3(3):282-290.
14. Aoki I, Takahashi Y, Chuang KH, et al. Cell Labeling for magnetic resonance imaging with the T1 agent manganese chloride. *NMR Biomed*. 2006;19(1):50-59.
15. Pautler RG, Silva AC, Koretsky AP. In vivo neuronal tract tracing using manganese-enhanced magnetic resonance imaging. *Magn Reson Med*. 1998;40:740-748.
16. Murayama S, Kato M. Photocontrol of biological activities of protein by means of a hydrogel. *Anal Chem*. 2010;82:2186-2191.
17. Murayama S, Jo J, Shibata Y, et al. The simple preparation of polyethylene glycol-based soft nanoparticles containing dual imaging probes. *J Mater Chem*. 2013;B1:4932-4938.
18. Murayama S, Ishizuka F, Takagi K, et al. Small-mesh-size hydrogel for functional photocontrol of encapsulated enzymes and small probe molecules. *Anal Chem*. 2012;84:1374-1379.
19. Murayama S, Nishiyama T, Takagi K, Ishizuka F, Santa T, Kato M. Delivery, stabilization, and spatiotemporal activation of cargo molecules in cells with positively charged nanoparticles. *Chem Commun*. 2012;48:11461-63.18.
20. Medina L, Reiner A. The efferent projections of the dorsal and ventral pallidal parts of the pigeon basal ganglia, studied with biotinylated dextran amine. *Neuroscience*. 1997;81(3):773-802.
21. Federle MP, Chezmar JL, Rubin DL, et al. Safety and efficacy of mangafodipir trisodium (MnDPDP) injection for hepatic MRI in adults: results of the U.S. multicenter phase III clinical trials (safety). *J Magn Reson Imaging*. 2000;12(1):186-197.
22. Gale EM, Atanasova IP, Blasi F, Ay I, Caravan PA. Manganese alternative to gadolinium for MRI contrast. *J Am Chem Soc*. 2015;137(49):15548-15557.
23. Serrano F, Deshazer M, Smith KD, Ananta JS, Wilson LJ, Pautler RG. Assessing transneuronal dysfunction utilizing manganese-enhanced MRI (MEMRI). *Magn Reson Med*. 2008;60(1):169-175.

**How to cite this article:** Eguchi Y, Murayama S, Kanamoto H, et al. Minimally invasive manganese-enhanced magnetic resonance imaging for the sciatic nerve tract tracing used intra-articularly administered dextran-manganese encapsulated nanogels. *JOR Spine*. 2019;2:e1059. <https://doi.org/10.1002/jsp2.1059>